Quaternary Science Reviews 312 (2023) 108152

Contents lists available at ScienceDirect

Quaternary Science Reviews

journal homepage: www.elsevier.com/locate/quascirev

Last interglacial seasonal hydroclimate in the North Sea–Baltic Sea region

S. Ni [a, b, 1, *], Z. Lu [b, c], Q. Zhang [d], J. Groeneveld [e, 2], K.L. Knudsen [f], M.-S. Seidenkrantz [f], H.L. Filipsson [a]

[a] Dept. of Geology, Lund University, Lund, Sweden
[b] Centre for Environmental and Climate Research, Lund University, Lund, Sweden
[c] Dept. of Physical Geography and Ecosystem Science, Lund University, Lund, Sweden
[d] Dept. of Physical Geography and Bolin Centre for Climate Research, Stockholm University, Stockholm, Sweden
[e] Center for Earth System Research and Sustainability, Institute for Geology, University of Hamburg, Hamburg, Germany
[f] Paleoceanography and Paleoclimate Group, and IClimate Centre, Dept. of Geoscience, Aarhus University, Aarhus, Denmark

ARTICLE INFO

Article history:
Received 30 November 2022
Received in revised form
21 May 2023
Accepted 22 May 2023
Available online xxx

Handling Editor: A. Voelker

Keywords:
The Last Interglacial
Seasonality
EC-Earth model
Insolation
Greenhouse Gas (GHG)
Hydrography
Data-model comparison
Baltic Sea
Paleoceanography
Temperature
Salinity
North Atlantic Oscillation (NAO)
Precipitation
Evaporation

ABSTRACT

The Last Interglacial (LIG) experienced substantial changes in seasonal insolation compared with the present day, which may have affected the hydrography and water-mass exchange in the North Sea and Baltic Sea region. Here we investigate the effects of solar radiation and greenhouse gas (GHG) forcing on the regional climate by analyzing model simulations of the LIG (127 ka BP), pre-industrial (PI, 1850 CE), and present-day (PD, 1990 CE) climates. We also interpret the reconstructed seasonal bottom water conditions using benthic foraminifera and geochemistry data.

Our simulations reveal that during the LIG, the Baltic Sea region (including the Kattegat and the Danish Straits) experienced more saline and colder bottom waters than those in the PD, in agreement with the reconstruction data. This can be attributed to lower GHG levels and enhanced water exchange of cooler, saline North Sea water into the Baltic Sea during the LIG. The thermocline was stronger during the summer months in the LIG, mainly due to the higher sea surface temperature (SST) compared to that of the PD resulting from increased summer insolation.

Further, the temperature anomalies (LIG–PD) show significant inverse correlations with the precipitation–minus–evaporation (P–E) at the Baltic Sea entrance. However, the P–E balance appears to have had minimal impact on salinity changes in the North Sea, the Baltic Proper, and the open sea area. Our findings indicate that monthly surface and bottom water salinity anomalies of LIG-PI exhibit strong positive correlations with the North Atlantic Oscillation (NAO) anomalies in the Baltic entrance region. During the LIG, a more positive phase of the NAO index in autumn played a crucial role in wind-driven major inflows and led to more intensive water exchange in the North Sea–Baltic Sea region compared to the late Holocene.

1. Introduction

The Last Interglacial (LIG, Eemian, 130–115 ka BP) was a distinct period in Earth's history, characterized by unique climate forcing compared to the present interglacial, known as the Holocene. The LIG period was one of the strongest anomalies in orbital forcing of the past one million years. During the LIG, greenhouse gas (GHG) concentrations were lower than those in the present-day (PD; 1990 CE) and similar to the pre–industrial (PI; 1850 CE) levels (Berger and Loutre, 1991; Laskar et al., 2004; Loulergue et al., 2008; Schilt et al., 2010; Schneider et al., 2013; Bereiter et al., 2015). However, our understanding of the LIG climate, particularly in the marine environment, remains limited due to the scarcity of precise reconstructions, especially in the Baltic Sea region. The combination of proxy–based reconstructions and model simulations of bottom–

* Corresponding author. Dept. of Geology, Lund University, Lund, Sweden.
E-mail address: sha.ni@uni-hamburg.de (S. Ni).
[1] present address: Institute for Geology, Hamburg University, Hamburg, Germany.
[2] present address: Institute of Oceanography, National Taiwan University, Taipei, Taiwan.

https://doi.org/10.1016/j.quascirev.2023.108152

and surface–water conditions provide the possibility to establish water column profiles of the past, which reflect water mass exchange and circulation (e.g., Adkins et al., 1997; Fronval et al., 1998; Galaasen et al., 2014). Moreover, some reconstructions based on proxy variables inform seasonal variations of seawater parameters, which greatly increases the accuracy of estimations (e.g., Cortijo et al., 1999; Brocas et al., 2016; Bova et al., 2021; Ni et al., 2021).

The North Sea–Baltic Sea waterway is crucial for the North Atlantic Ocean, connecting the world's largest inland brackish–water sea to the North Sea and ultimately the Atlantic Ocean. The major inflows from the Atlantic and North Sea saline water into the Baltic Sea renew its deep water. These saline water inflows and brackish water outflows are largely hindered by the complex topography in the transition area between the North Sea and the Baltic Sea (Schrum and Backhaus, 1999). Thus, the North Sea–Baltic Sea waterway greatly influences the water mass exchange (Lambert et al., 2016, 2018; Winsor et al., 2001) and density changes in the North Sea and the North Atlantic, potentially impacting the global thermohaline circulation (Kuhlbrodt et al., 2007; Lambert et al., 2018).

The North Atlantic Oscillation (NAO) plays a vital role in shaping the climate in Europe, affecting winter temperatures and precipitation in the North Atlantic and northern European regions (e.g., Hurrell, 1995; Lu and Greatbatch, 2002; Mariotti and Arkin, 2007; Trigo et al., 2002). A negative NAO phase during winter corresponds to weaker westerly winds and more easterly/northeasterly winds, leading to colder, drier conditions and reduced precipitation in northern Europe. In contrast, a positive NAO phase is linked to stronger westerly winds during winter, substantially increasing water inflow from the North Sea into the Baltic Sea (Lehmann and Hinrichsen, 2001). This increases the Baltic Sea salinity, particularly following a strong negative NAO phase, during which easterly winds drive a robust outflow of the Baltic Current, resulting in a water level deficit in the Baltic Sea relative to the North Sea (Lehmann and Hinrichsen, 2001). In addition, a tendency towards the high–index state of the NAO may amplify the seasonal cycle (Felis et al., 2004). The LIG, characterized by a stronger North Atlantic Drift and an overall warmer climate, could have experienced a more consistently positive NAO than today, potentially even more pronounced than during the Medieval Climate Anomaly (e.g., Seidenkrantz et al., 2007; Olsen et al., 2012; Trouet et al., 2012; Sicre et al., 2014). Model simulations can be employed to explore the NAO's influence on the LIG climate. Unfortunately, fully coupled climate models focusing on the hydrological conditions in the North Sea–Baltic Sea region further back in time are still scarce. Nevertheless, some studies have successfully simulated Baltic climate and hydrography on time scales of a millennium or shorter (e.g., Humborg et al., 2000; Hansson and Gustafsson, 2011; Schimanke et al., 2012).

In this study, we used a fully coupled Earth–System Model EC–Earth3–LR to examine the influence of solar radiation and GHG forcing on regional climate changes during the LIG. We analyzed the simulated climate responses to atmospheric–oceanic interactions, ocean circulation, thermocline changes, and hydrographic variables, such as seawater temperature and salinity in the Baltic Sea–North Sea region. We compared the climate response to orbital and GHG forcing between the LIG (enhanced orbital forcing) and the PI (1850 CE, pre–industrial control experiment), as well as the PD (1990 CE, present-day) to understand the impact of these factors on regional environmental changes. In particular, we focused on exploring changes in seasonality resulting from insolation differences during the LIG compared to the PD.

Furthermore, we investigated the role of GHG in affecting regional climate by comparing conditions during the PI and PD (present day, 1990 CE, with increased GHG levels compared to those in the PI). The differences between the anomalies of LIG–PD and LIG–PI highlight the effect of greenhouse gas concentration on the climate. Finally, we compared the LIG proxy-based reconstructions and simulations with the PD observations and transient simulations respectively, to evaluate the model performance in simulating the LIG climate. This comparison will help identify the model limitations and provide valuable information for predicting future regional environmental changes using a general circulation model.

2. Methods and settings

2.1. Earth system model (ESM) simulations

We employed a state-of-the-art, fully coupled European community Earth-System Model EC-Earth3-LR with active atmosphere, ocean, sea-ice, and land components (Lu et al., 2021; Zhang et al., 2021; Döscher et al., 2022). The model features a spatial resolution approximately $1 \times 1^{\circ}$ for the atmosphere and land, while the ocean/sea–ice model operates at a standard resolution of about 1°. We performed three snapshot simulations: 1) an early LIG time slice with boundary conditions at 127 ka BP (LIG), 2) the present day (1990 CE, PD), and 3) a pre–industrial period (1850 CE, PI) as a control simulation (Zhang et al., 2021; Lu et al., 2021).

The three experiments allow us to examine the effects of orbital configuration and greenhouse gas (GHG) concentration separately by comparing the PI and the PD to the LIG simulations. Boundary conditions of the simulations (Table 1) were prescribed following the Paleoclimate Modeling Intercomparison Project (PMIP4) protocol (Otto-Bliesner et al., 2017). For the LIG simulations, the model computes the orbital parameters at 127 ka BP following Berger (1978). The GHG (CO_2, CH_4, and N_2O) concentrations in the LIG simulation are based on Antarctic ice cores (Loulergue et al., 2008; Schilt et al., 2010; Schneider et al., 2013; Bereiter et al., 2015). The land–sea mask and solar constant remain the same as those in the PI. Significant differences in GHG levels exist between the LIG and PD experiments. LIG-PD anomalies reflect the combined impact of GHG levels and the orbital configuration as external forcing. Since the orbital configuration is similar for both PI and PD simulations, the major differences in external forcing between PI and PD are due to GHG levels. Therefore, we could compare the differences between LIG-PI and LIG-PD anomalies to assess the impact of GHG levels on the climate.

The LIG and PI simulations are documented and evaluated by Zhang et al. (2021). Equilibrium state criteria are defined by a global mean surface temperature trend of less than 0.05 °C per century and a stable Atlantic meridional overturning circulation (AMOC), although the deep ocean may need more time to be at equilibrium.

Table 1
Boundary conditions of the simulations.

Period	Eccentricity	Obliquity (°)	Perihelion − 180	CO_2 (ppm)	CH_4 (ppb)	N_2O (ppb)
1990 CE/PD	0.016708	23.440	102.72	352.9	1705.6	307.8
1850 CE/PI	0.016764	23.549	100.33	284.3	808.2	273.0
127 ka BP/LIG	0.039378	24.040	275.41	275	685	255

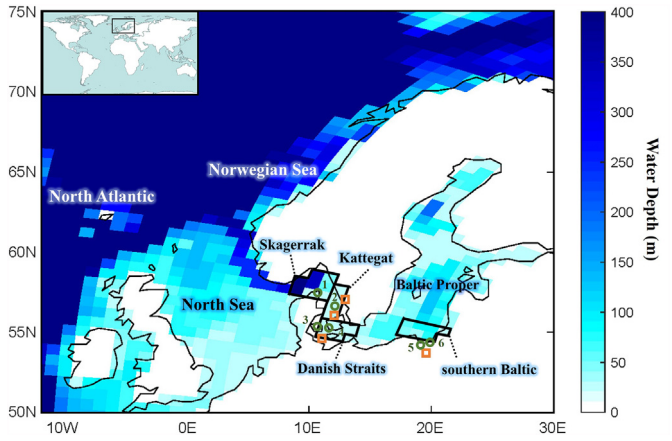

Fig. 1. Land–sea mask of the study area with water depth (m) used in the model for three simulations. The eight regions for model simulations: the North Atlantic, the Norwegian Sea, the North Sea, and the Baltic Proper; in the North Sea – Baltic Sea waterway: the Skagerrak, the Kattegat, the Danish Straits, and the southern Baltic Sea are marked by black squares. The proxy-based reconstructions of bottom water conditions in the Baltic region (Ni et al., 2021; the Skagerrak: 1 Åsted Vest; the Kattegat: 2 Anholt; the Danish Straits: 3 Mommark, 4 Ristinge; the southern Baltic: 5 Licze, 6 Obrzynowo) are indicated by green circles with numbers. The proxy-based reconstructions of sea surface conditions in the Baltic region (Burman and Påsse, 2008; Funder et al., 2002) are indicated by orange squares. Sites for the proxy-based reconstructions are on land now due to a higher sea level during the LIG.

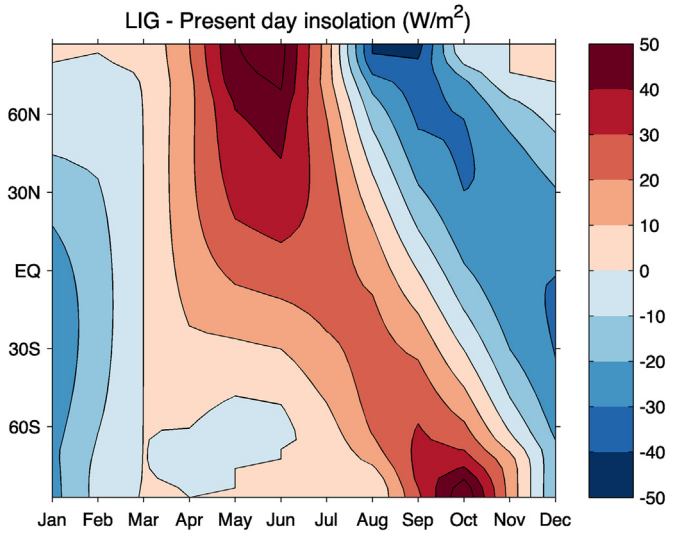

Fig. 2. Monthly insolation anomalies of LIG–PD, monthly insolation curve at 55°N for this study see Supplementary Fig. 1.

The LIG simulation reached quasi-equilibrium after 200 years starting with initial conditions from an equilibrated PI control (Zhang et al., 2021). The PD simulation reached equilibrium after a 150-year spin–up. Our analysis is based on 200 years of climate mean data.

We examined the precipitation–minus–evaporation (P–E) for the study area (Fig. 1) and the NAO index to investigate the underlying forcing mechanisms behind the regional hydrographic changes in the North Sea–Baltic Sea. The NAO index for each simulation was calculated using the simulated mean Sea–Level Pressure (SLP) differences between grid cells near Iceland (28°W, 64°N) and the subtropical Atlantic station Azores (9°W, 38°N), as described by Caian et al. (2018), based on the modern NAO index definition. We assume that the Icelandic low-pressure centre and the Azores high-pressure centre used for NAO index calculation remain the same across different simulations. We normalized each SLP value by subtracting the mean value and dividing it by the standard deviation. We assessed the P–E, ocean temperature, and salinity from the model output for various regions in northern Europe (the North Atlantic, the Norwegian Sea, the North Sea, the Skagerrak, the Kattegat, the Danish Straits, the southern Baltic, and the Baltic Proper) to investigate the interaction between environmental factors and hydrographical changes in these regions. The Kattegat and Danish Straits serve as the transition zone between the North–Baltic Sea, while the southern Baltic Sea and the Baltic Proper represent the Baltic Sea region.

Solar radiation at ~55°N (Fig. 2) exhibits a positive anomaly during spring (March–April–May; MAM) and summer (June–July–August; JJA), while it is lower from August to November in the LIG compared to the PD.

2.2. Modern conditions

We used monthly monitoring hydrographic data from four regions along a transect stretching from the eastern North Sea to the southern Baltic Sea, namely the Skagerrak, the transition zone (the Kattegat and the Danish Straits) between the Skagerrak and the Baltic, and the southern Baltic Sea. We compared this data to proxy-based reconstructed values for the LIG scenario. The transition zone connects the relatively open marine area (the North Sea and the Skagerrak) to the brackish Baltic Sea environment, with salinities gradually decreasing from NW to SE. Mean salinities in the North Sea are around 34 due to its open connection with the North Atlantic Ocean, while Baltic Sea salinities in the upper and central water column are typically below 8 (Schrum and Backhaus, 1999; HELCOM, 2018).

We used hydrographic data from 1990 CE (Fig. 1, Baltic Nest Institute (BNI) Stockholm University Baltic Sea Centre). Representative water depths for surface and bottom waters were chosen based on paleo-water depth estimates (Ni et al., 2021). Surface water was defined as shallower than 10 m, while bottom water ranged from below the halocline to the seafloor, i.e., 25–90 m in the Skagerrak, 20–80 m in the Kattegat, 15–25 m in the Danish Straits, and 15–20 m in the southern Baltic Sea. In 1990, the largest monthly difference between August and December SST (at about 1 m water depth) in the Skagerrak was ~14 °C, while the differences were ~12, ~15, and ~15 °C in the Kattegat, the Danish Straits, and the southern Baltic, respectively. The highest SSTs occurred in August, reaching 17–20 °C, whereas the warmest bottom water conditions appeared one or two months later, in September or October. A similar time lag occurs for the lowest water temperatures; with the lowest surface water temperatures occurring from December to January and the lowest bottom water temperatures from January to February. The largest vertical temperature difference in the water column occurred in summer (i.e., June and July), while during winter and early spring, the differences were fairly small (less than 1 °C).

In 1990, the largest vertical salinity gradient in the water column occurred in May, with a surface–bottom salinity difference of ~7 and ~18 in the Skagerrak and the Kattegat, respectively. In the Danish Straits, the salinity gradient was 7–10 during May and July. The salinities of surface and bottom water in the southern Baltic Sea were very similar, indicating a brackish water environment with no vertical gradient. Today, the saline water inflow from the Skagerrak and brackish water outflow from the Baltic Sea meet in the Kattegat, resulting in a strong halocline at 15–20 m water depth and with the largest salinity gradient in the transition zone.

2.3. Data-model comparison

We present a data-model comparison to evaluate the differences of the impact of LIG climate on the North Sea–Baltic Sea region. For this comparison, we used quantitative proxy-based LIG reconstructions (LIG_{proxy}) and modern hydrographic monitoring data (PD_{obs}). Meanwhile, for model simulations, we used the equilibrium climate states of the LIG (Zhang et al., 2021) and transient PD simulations over 1976–2005 ($PD_{transient}$) with a time-varying GHG forcing (accessed from the Earth System Grid Federation, ESGF). The monitoring hydrographic data for 1990 CE (PD_{obs}) and simulations for 1976–2005 CE ($PD_{transient}$) can be expected to represent the transient evolution of the climate system. Therefore, we compared proxy-data (LIG_{proxy}-PD_{obs}) and model-simulations (LIG-$PD_{transient}$) to identify the forced responses in the climate system. We focused on the proxy-based reconstruction and monthly mean model output of seawater temperature and salinity of the North Atlantic–Baltic Sea region. Note that this approach is different from model-model comparison (between different periods LIG, PI and PD) as all the snapshot simulations are in an equilibrium (not transient) state for a fair comparison.

Quantitative proxy-based reconstructions (LIG_{proxy}) for bottom water conditions in the North Sea–Baltic Sea area during the Last Interglacial period are scarce. Here, we collected available early LIG (128–126 ka BP) datasets based on benthic foraminiferal geochemistry (magnesium/calcium and stable oxygen isotopes) from six sites in the Skagerrak–Baltic Sea region: the Skagerrak: site Åsted Vest; the Kattegat: site Anholt; the Danish Straits: sites Mommark and Ristinge; the southern Baltic: sites Licze and Obrzynowo (see numbered green circles in Fig. 1; Ni et al., 2021). We compared these data with the simulated bottom water conditions (LIG).

The quantitative reconstructions were based on geochemical analyses of three benthic foraminiferal taxa/groups (the Skagerrak and the Kattegat: *Bulimina marginata*; the Danish Straits and the southern Baltic Sea: *Ammonia batava* and *Elphidium clavatum–selseyensis*) that represent summer and spring bottom water conditions. These available data provide seasonal bottom water estimations for comparison and improvement of model simulations. Sea surface temperature and salinity data are available based on *Littorina littorea* (common periwinkle) gastropod geochemistry and mollusc fauna reconstructions in the Kattegat and the southern Baltic region at 125 ka BP (Burman and Påsse, 2008; Funder et al., 2002). The qualitative estimations were based on mollusc assemblages, dominated by species such as *Nassarius reticulatus*, *Ostrea edulis*, and *Timoclea ovata* (cf. Burman and Påsse, 2008; Funder et al., 2002).

3. Results

3.1. Simulated water temperature and salinity

3.1.1. The last interglacial (LIG) compared with modern (PD) conditions

We examined the simulated monthly sea surface and bottom water temperatures and salinities to compare the LIG (i.e., 127 ka BP) and the modern climate (PD, 1990 CE). Our analysis focused on four study regions (the Skagerrak, the Kattegat, the Danish Straits, and the southern Baltic Sea) in the North Sea–Baltic Sea transition zone (Fig. 3) and four study regions in the North Atlantic Ocean, Norwegian Sea, North Sea, and the Baltic Proper (Fig. 4).

During the LIG, the surface water temperature exhibited a more pronounced seasonality compared with that of the PD. The model reveals higher sea surface temperatures (SSTs) from June to September and lower SSTs in other months for the North Sea–Baltic Sea region during the LIG than those during the PD. It also shows a lower spring and a similar/slightly lower summer bottom–water temperature (BWT) in the LIG. Temperature anomalies (LIG-PD) increased along the transition zone outside the Baltic Sea to the Baltic Proper. The difference between SST and BWT was larger in the summer of the LIG than today across our study region (Supplementary Fig. 2).

Notably, the maximum SST anomalies (LIG–PD) of about 2 °C in the North Sea, the Skagerrak, the Kattegat, and the Danish Straits occurred during summer. In the southern Baltic and the Baltic Proper the maximum anomalies reached ~4 °C, while in the North Atlantic and the Nordic Sea, the anomalies were smaller, at around 1 °C (Fig. 4). The BWT anomalies for all months and locations included in our study indicate that the LIG bottom water was cooler than that of the PD. The BWT anomalies in the transition area (i.e., the Kattegat and the Danish Straits) display stronger seasonal variations (Fig. 3) due to the relatively shallow water depth, whereas inside the Baltic Sea and outside the Skagerrak to the open ocean, the BWT anomalies were more stable throughout different seasons (Fig. 4).

In the relatively shallower transition zone and the southern Baltic, simulated surface- and bottom-water salinities indicate large differences in seasonality (Fig. 3). From the Kattegat to the Baltic Proper, the LIG annual mean salinities were consistently higher than those of the PD period by 0.4–1.9. However, outside the Baltic Sea, salinity ranges for both the LIG and the PD were quite similar, between −0.4 and −0.1. The surface water salinities (SSSs) were significantly lower between May and September compared to colder months during both the LIG and the PD in the transition zone. In contrast, bottom water salinities (BWSs) show no significant seasonal difference, except in the Danish Straits, where higher summer and early autumn BWS led to a more pronounced halocline for both the LIG and the PD.

The annual mean salinity anomalies were more pronounced in the surface water than in the bottom water in the Skagerrak-Kattegat-Baltic Sea. These anomalies increased along the transect from the transition zone to the Baltic Proper (Fig. 5). In the Skagerrak, the Kattegat, and the Danish Straits, the SSS annual anomalies were ~1 larger than BWS anomalies. In the Baltic Proper and the southern Baltic Sea, the differences between SSS and BWS anomalies were smaller (~0.5). Outside the Skagerrak, there was no significant difference between the SSS and BWS anomalies in the water column.

In the transition zone (i.e., the Skagerrak, the Kattegat, and the Danish Straits), the SSS anomalies were less positive in August and September compared to other months. The BWS anomalies show no significant seasonality from the Skagerrak to the North Atlantic Ocean. From the transition zone to the southern Baltic Sea, the shallower water depth contributed to larger seasonal variations in BWS anomalies. This resulted in a salinity difference of up to 1 between summer (i.e., July) and winter (i.e., February).

3.1.2. The last interglacial (LIG) compared with the pre-industrial (PI) conditions

The model responded with a higher mean temperature and salinity in the Baltic Sea in the LIG than in the PI simulation. There was also a larger seasonality in the surface waters during the LIG (Fig. 6). The anomalies of SST and BWT were generally higher compared with the LIG–PD anomalies. During the LIG, summer SSTs were significantly higher than those in PI, with anomalies reaching up to 7 °C in the Baltic Proper. The temperature anomalies (LIG–PI) were consistently positive, indicating a warmer water column during the LIG compared to that of the PI (Fig. 6). The SST anomalies in the LIG were much higher during the summer months, up to 5–6 °C than in other months. The BWT, however,

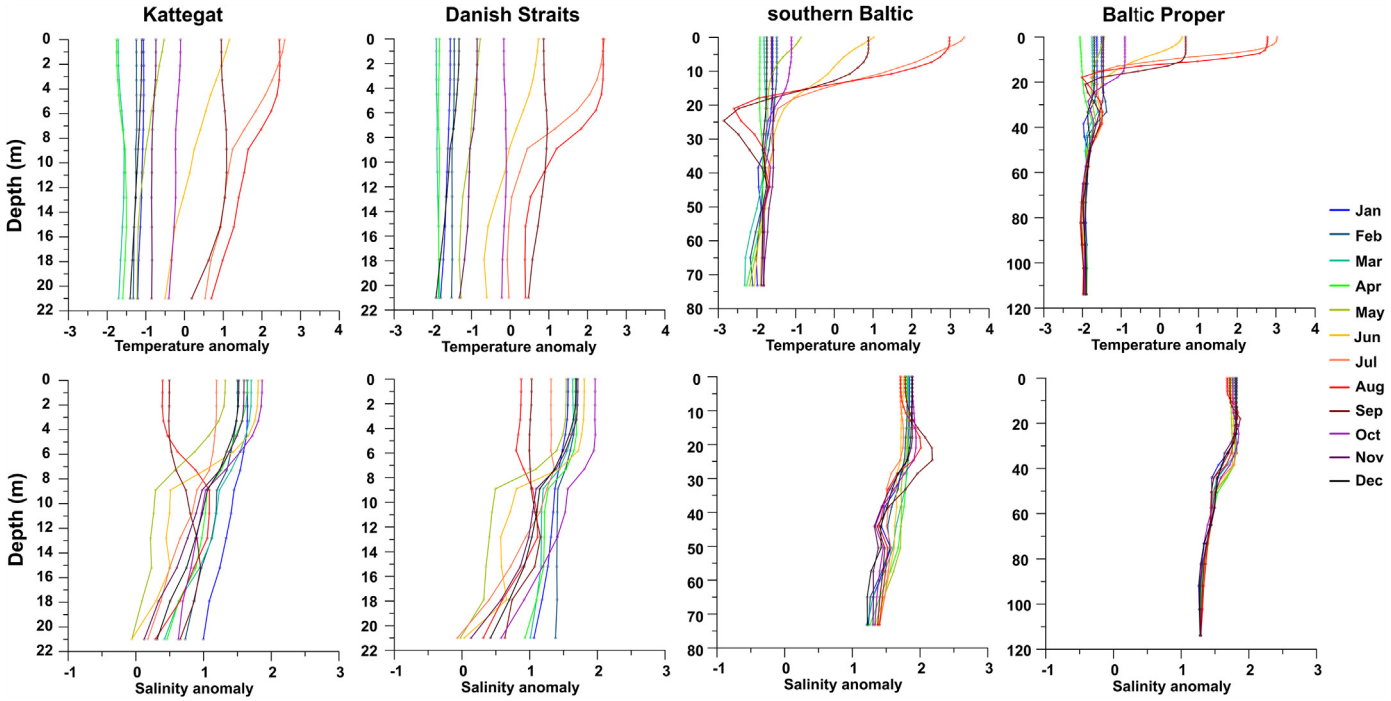

Fig. 3. Simulated monthly temperature [°C] and salinity [PSU] anomalies: the LIG 127 ka BP minus PD (1990 CE), at four locations in the transition zone (i.e., the Kattegat and the Danish Straits) and the Baltic Sea (Fig. 1).

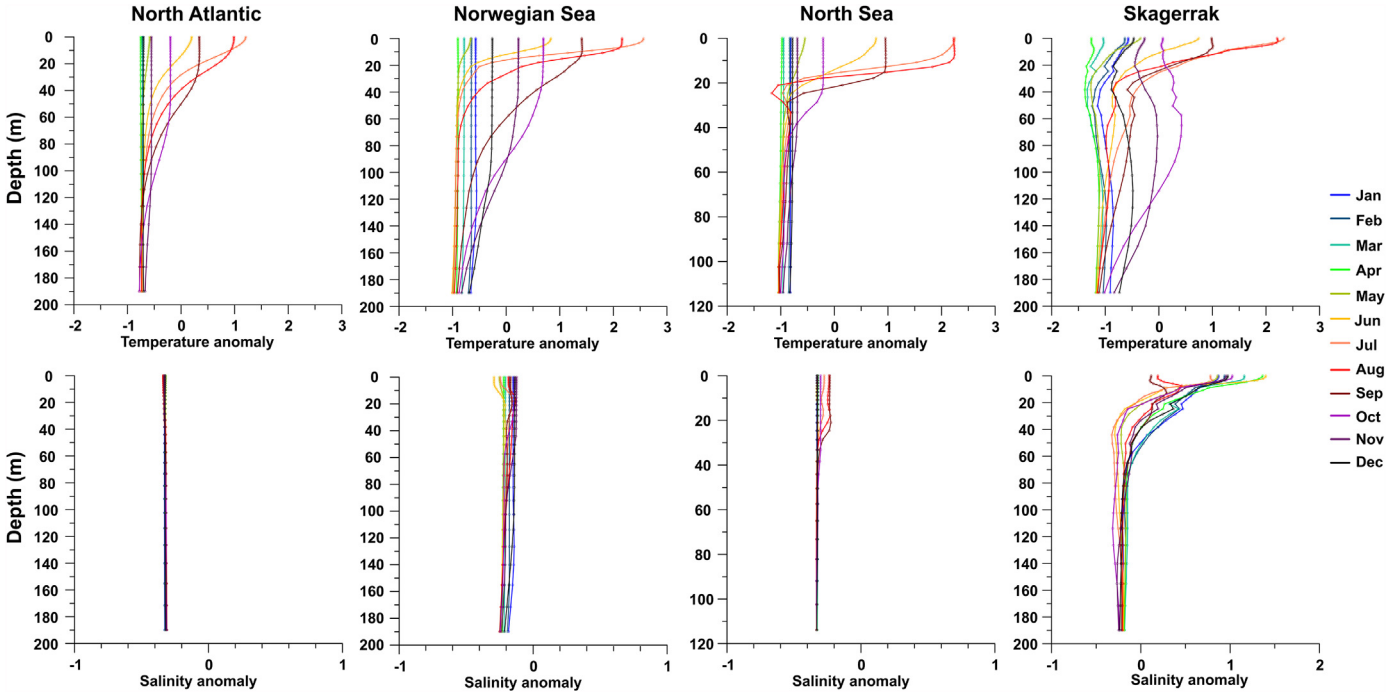

Fig. 4. Simulated monthly temperature [°C] and salinity [PSU] anomalies: the LIG 127 ka BP minus PD (1990 CE), at four locations in the North Atlantic to the Skagerrak.

shows no seasonal variation due to a greater water depth in the North Atlantic–North Sea region and the Baltic Proper, while in the transition zone, there was a seasonal variation.

The SSS and BWS were generally higher during the LIG than those during the PI in the Danish Straits and the Baltic Sea (Fig. 6). The mean salinity anomalies (LIG–PI) increased along the Skagerrak-Kattegat-Baltic Sea. The seasonal variations were relatively higher in the Skagerrak, the Kattegat, and the transition zone, suggesting that in the more open-marine conditions and within the Baltic Sea, salinity anomalies did not exhibit significant seasonal variability. The seasonal variation amplitude of SSS anomalies was higher than the BWS anomalies. However, we observed no significant difference between the means of SSS and BWS anomalies across all the regions.

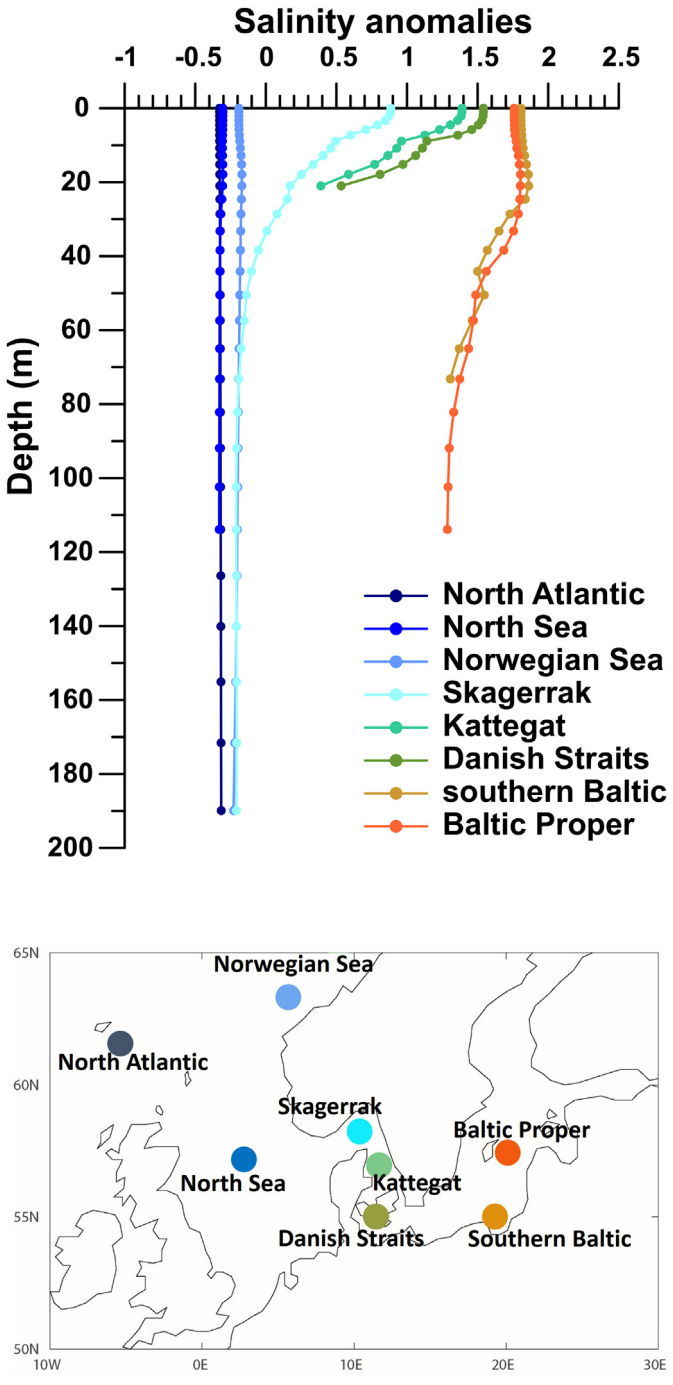

Fig. 5. The annual mean salinity anomalies in the water column (LIG–PD) in eight locations in the region of the North Atlantic and the Baltic Sea.

3.2. Simulated precipitation–minus–evaporation (P–E), NAO index and sea-ice

The difference between precipitation and evaporation (precipitation–minus–evaporation, P–E) shows different seasonal variations across various study areas during both the LIG and the PD (Fig. 7). The annual P–E of the LIG was significantly lower than that of the PD in all the regions. The LIG P–E values were mostly negative, indicating dry conditions, during summer and early autumn in the transition zone and the Baltic Proper. The North Atlantic, North Sea, and Norwegian Sea regions experienced positive P–E values, suggesting wet conditions during summer and early autumn. P–E anomalies (LIG–PD) in different regions show different seasonal variations (grey lines in Fig. 7). In the region Skagerrak-Baltic, P–E anomalies were more negative during summer and early autumn compared to other months, while in open sea regions like the North Atlantic, North Sea and Norwegian Sea, P–E anomalies were less negative.

The annual mean P–E values for the LIG and the PI demonstrate no significant difference in most study regions, except for the transition zone (the Kattegat and the Danish Straits). In these areas, the PI P–E values were higher than those of the LIG (Fig. 7), indicating dryer conditions during the LIG than during the PI. The seasonal P–E variations of the LIG and the PI show no significant difference in any regions.

Monthly mean SLP near the Azores and Iceland shows different seasonal variations. Near the Azores, the SLPs were comparatively lower during summer compared to other seasons, while near central Iceland, the SLPs were relatively higher in the middle of the year. The NAO index shows a negative phase from April to August (October) during the LIG (PD) simulations (Fig. 8), and a positive phase from September (November) to March. No significant seasonal variation was observed for the NAO index anomalies (LIG–PD), which fell within the range of ±0.5, except for the October NAO index in the LIG, which was significantly higher than that in the PD. The PI NAO index displays no difference in variation compared to the PD. There was no significant difference in the variation or mean of the NAO index between the LIG and the PD periods or between the LIG and the PI periods (Supplementary Fig. 3). Similarly, the NAO index anomalies LIG–PD and LIG–PI show no significant difference.

During the winter months, sea-ice coverage in the Baltic Sea was higher in the PI compared to the LIG and the PD (Supplementary Fig. 4a), while the LIG and the PD periods had similar sea-ice extent. No significant difference was found in the annual mean sea-ice extent and thickness within the Baltic Sea across the three periods. The sea-ice thickness anomaly (LIG-PD) shows thicker sea-ice (Supplementary Fig. 4b), therefore, the sea-ice volume was larger in the Arctic region during the PD compared with that of the LIG.

4. Discussion

4.1. Variations in seasonal seawater conditions in the North Sea–Baltic Sea region

The EC-Earth model simulations reveal a more pronounced seasonality in seawater temperatures (both SST and BWT) during the LIG compared to the PD. This finding aligns with the simulated continental temperatures with the ECHO–G model (Kaspar et al., 2005) and is attributed to the increased summer and decreased winter insolation during the LIG (Laskar et al., 2004). Notably, higher insolation during the LIG was observed from April to July, leading to a roughly two-month delay in surface seawater warming. In the LIG, the differences between SST and BWT in all regions were significantly larger than those in the PD during the warm months (Supplementary Fig. 2), suggesting a stronger thermocline during the warm season in the LIG. However, the simulated depths of the thermocline show no significant difference between any two periods (i.e., LIG–PI or LIG–PD).

The differences between BWS and SSS anomalies (LIG–PD) in the warm season were higher than in the cold season, indicating a stronger halocline during the summer months at most of the locations (Supplementary Fig. 5). In the transition zone, SSS anomalies were larger than BWS anomalies when comparing the LIG to the PD, meaning the salinity differences between the surface and

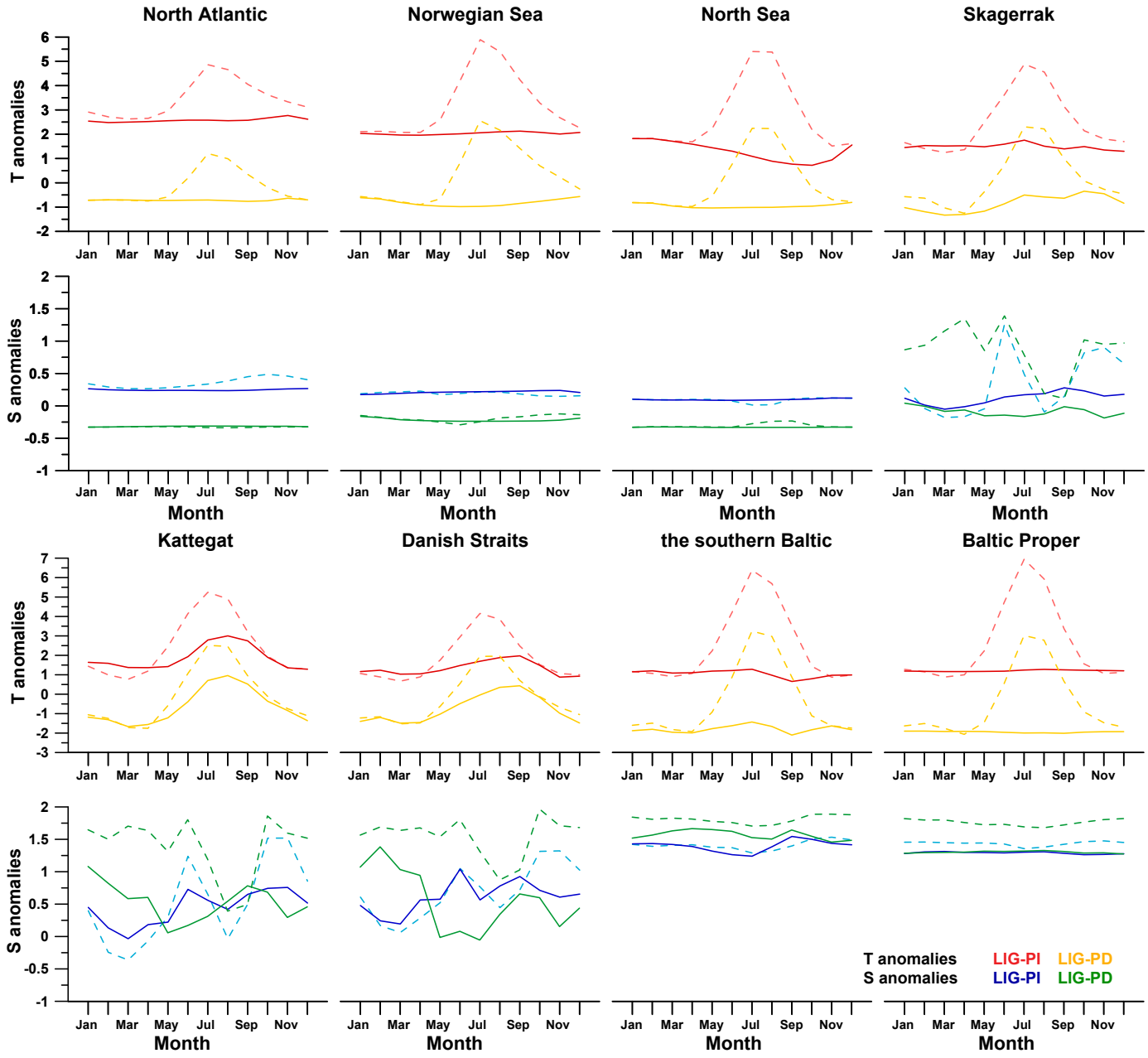

Fig. 6. Simulated monthly temperature [°C] and salinity [PSU] anomalies: the LIG 127 ka BP minus PI and the LIG minus PD, at eight locations in the North Atlantic, the Norwegian Sea, the North Sea, the Skagerrak, the transition zone (i.e., the Kattegat and the Danish Straits) and the Baltic Sea (i.e., the southern Baltic and the Baltic Proper). Dashed lines indicate the surface water, whereas solid lines indicate the bottom water at each location. Different colors indicate temperature and salinity anomalies of LIG-PI and LIG-PD.

bottom water were smaller during the LIG. This can be attributed to higher SSS caused by an increased inflow of North Atlantic surface water and drier conditions with lower P−E during the LIG compared to that during the PD. The halocline was notably weaker in the LIG than in the PD, particularly in the transition zone and the Baltic Sea region, as evidenced by the smaller salinity differences between BWS and SSS. Annual salinity anomalies in different regions reveal positive anomalies in the transition zone, which follows the pathway from the Skagerrak through the Kattegat and the Danish Straits (Fig. 5). This suggests that the saline waterfront, where marine water mixes with brackish water, had expanded further into the Baltic Sea during the LIG. Consequently, more significant inflow events led to higher salinity in the southern Baltic and deep water renewal in the Baltic Proper.

The densities of the seawater in the LIG were greater than those in the PD in the transition zone (Kattegat and the Danish Straits) and the Baltic Sea, while in the North Atlantic, the North Sea and the Norwegian Sea, the densities were the opposite (Fig. 9). The calculations (density of Standard Mean Ocean Water, ρSMOW) were based on temperature and salinity (Massel, 2015, Eq. A0.2). The density anomalies (LIG−PD) were larger during cold season compared to warm season (July, August, and September) in the transition zone. This can be attributed to a higher temperature and lower salinity in the LIG during the warm season. As a result, the LIG exhibited a more distinct seasonal variation in the pycnocline – a layer in the ocean where water density changes rapidly - compared to the PD in the transition zone and the Baltic Sea. This led to a stronger pycnocline in July and August, and a weaker one in the

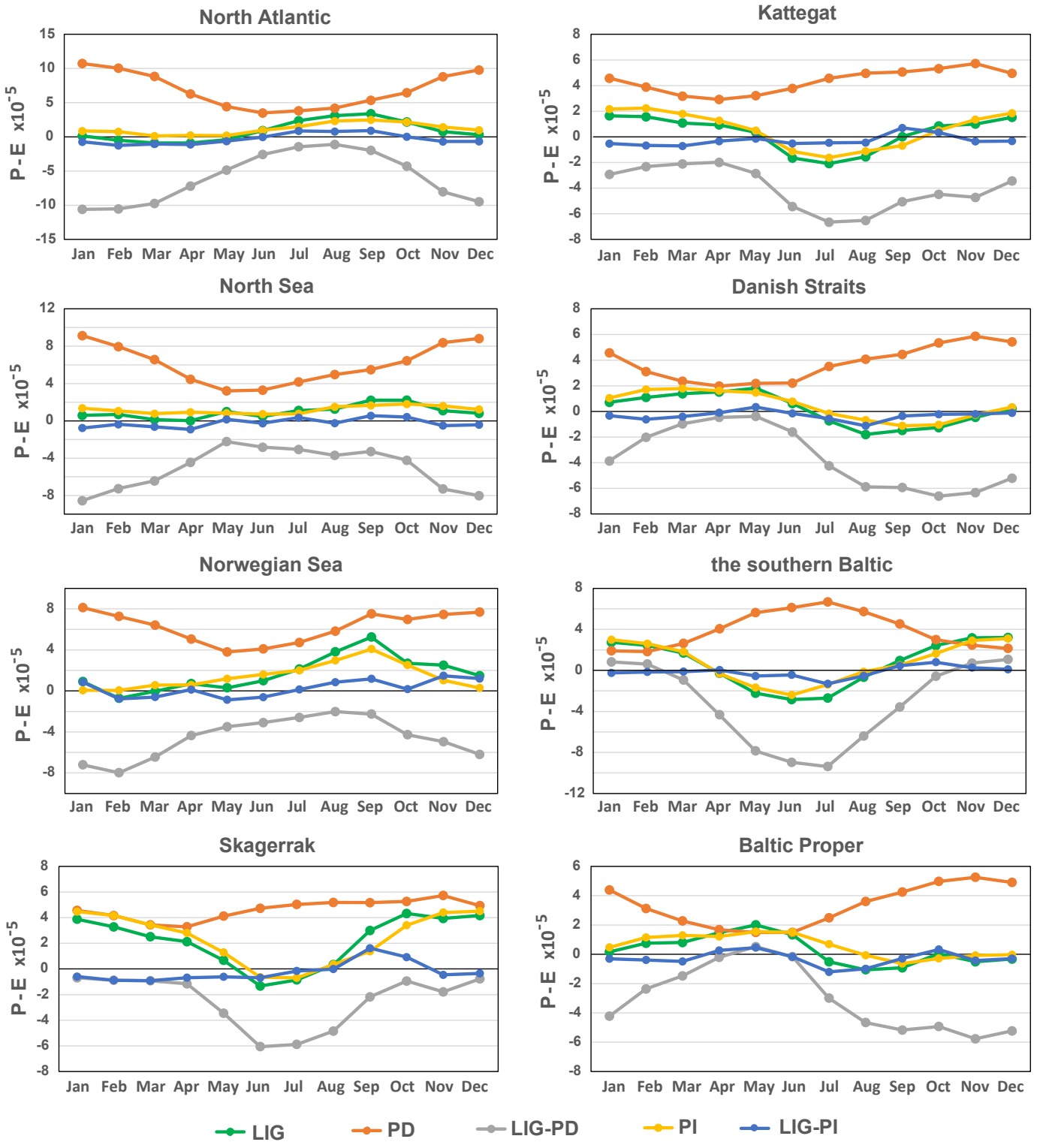

Fig. 7. Simulated monthly P−E of LIG 127 ka BP, PD 1990 CE and PI 1850 CE (green, orange and yellow lines, respectively), P−E anomalies of LIG−PD and LIG−PI (grey lines and blue lines, respectively) in the eight regions.

remaining months. The intensified pycnocline during the warm months (July to September) in the LIG likely contributed to a greater stratification of the water column in the coastal area of the Baltic Sea, especially in the area with shallower water depth or warmer bottom water, such as Kattegat and Mommark site in the Danish Straits. This increased stratification could have resulted in seasonal hypoxia in the bottom water, causing stress on marine life. Evidence of this stress can be found at the Mommark site, where high levels of benthic foraminiferal flux (Kristensen and Knudsen, 2006), increased Mn/Ca ratios in benthic foraminifera (Ni et al., 2021), and

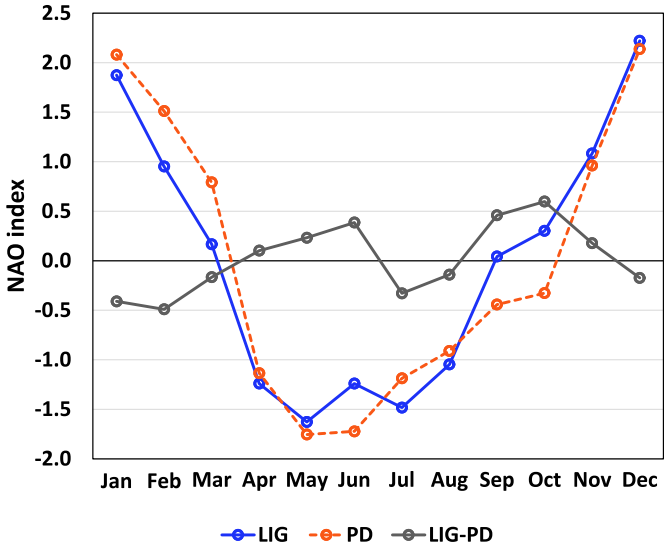

Fig. 8. Simulated monthly NAO index based on sea level pressure near the Azores and Iceland of LIG, PD, and LIG-PD anomalies.

an abundance of hypoxia tolerant mollusc fauna (Funder and Balic-Zunic, 2006) were observed. These findings suggest the presence of bottom water oxygen stress and hypoxic bottom water conditions, which agrees with the results of our model simulation.

4.2. Comparison of reconstructed and simulated results

4.2.1. Temperature

The BWT reconstructions (mean values of a time slice between 128 and 126 ka BP) agree with the simulations by indicating lower LIG spring and summer BWT at ~127 ka BP compared to the modern observations in 1990 CE (PD_{obs} for proxy-based results) and the $PD_{transient}$ (1976–2005 CE) transient simulations ($PD_{transient}$ for model simulations, supplementary Fig. 6) in the transition zone and the southern Baltic Sea sites. The reconstructed LIG spring BWTs were 0–4 °C lower than the PD_{obs} spring BWTs in these areas, while the LIG summer BWTs were 1–4 °C lower. The proxy reconstructions show higher amplitudes of BWT anomalies than the simulation in the Danish Straits (spring) and the southern Baltic Sea (summer), but lower in the Skagerrak and Kattegat (spring, Fig. 10). Both the proxy data and model simulation suggest that the bottom water was cooler during the LIG.

The summer SST estimates also support the result that the LIG SST was higher than in modern times. However, the reconstructed SST based on gastropod $\delta^{18}O$ shows temperatures up to ~12 °C higher during the LIG's warmest season (Burman and Påsse, 2008), which is significantly higher than the simulated LIG-$PD_{transient}$ differences. These differences may be due to the uncertainty in the gastropod $\delta^{18}O$-based temperature calculation using a fixed salinity estimate (29 PSU), as well as the use of modern bathymetry and sea-level settings in the model, or the limitations of the global model in capturing the effects of the wider and deeper connection to the North Sea during the LIG. Moreover, the coastal proxy data are heavily influenced by water depth, with the global models may not accurately represent at high resolutions. The comparisons of proxy reconstructions of SST and terrestrial temperature to simulations for 125 ka during the LIG on a European or global scale also indicate a generally warmer climate during the LIG than during the PI (Kaspar et al., 2005; Otto–Bliesner et al., 2013). Notably, the SST anomalies during summer were higher than those during winter.

Both model simulations and proxy reconstructions reveal higher SST and lower BWT during the LIG summer. This suggests a stronger seasonal thermocline in the water column in the transition zone and the southern Baltic Sea during the LIG. The Danish Strait, however, shows no significant difference in summer mean BWT between the LIG and the $PD_{transient}$, which could also be due to

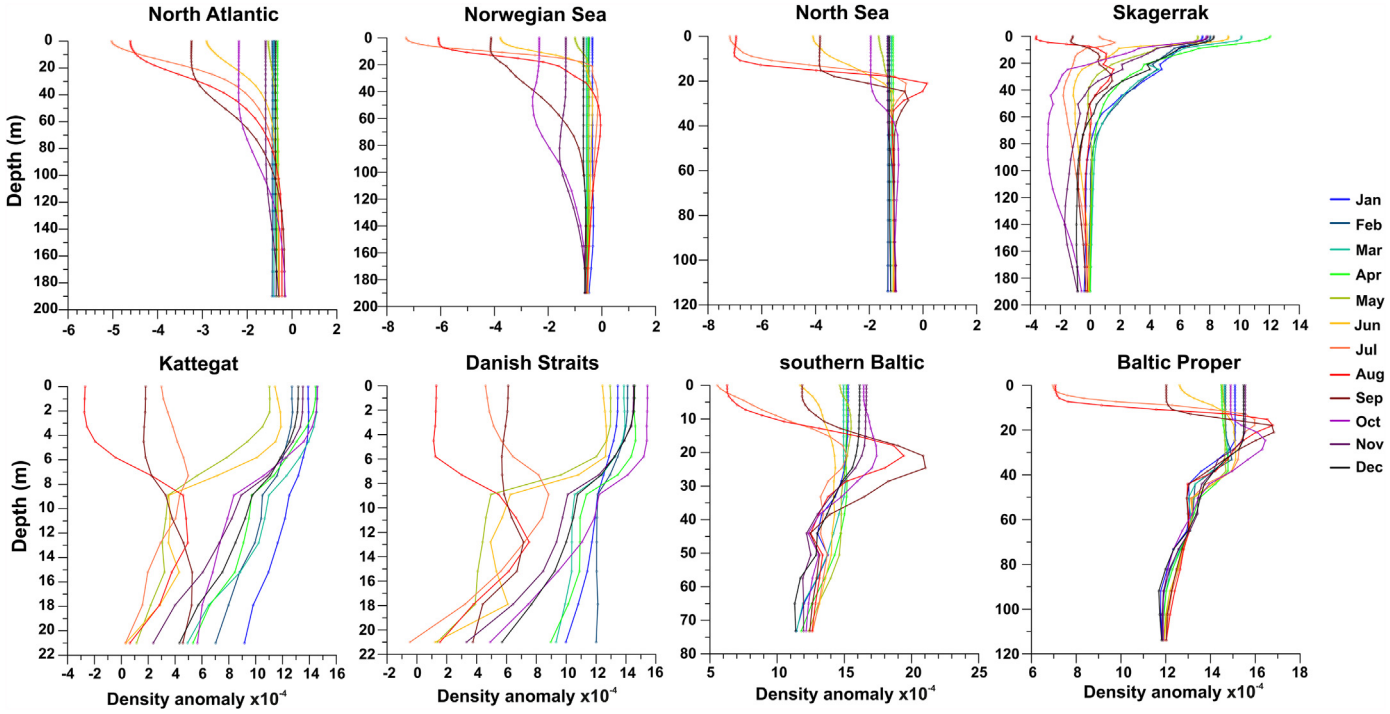

Fig. 9. Calculated monthly seawater density (ρSMOW) anomalies based on temperature and salinity simulations: LIG 127 ka BP minus PD (1990 CE) at locations in the North Atlantic to the Skagerrak and the transition zone to the Baltic Proper.

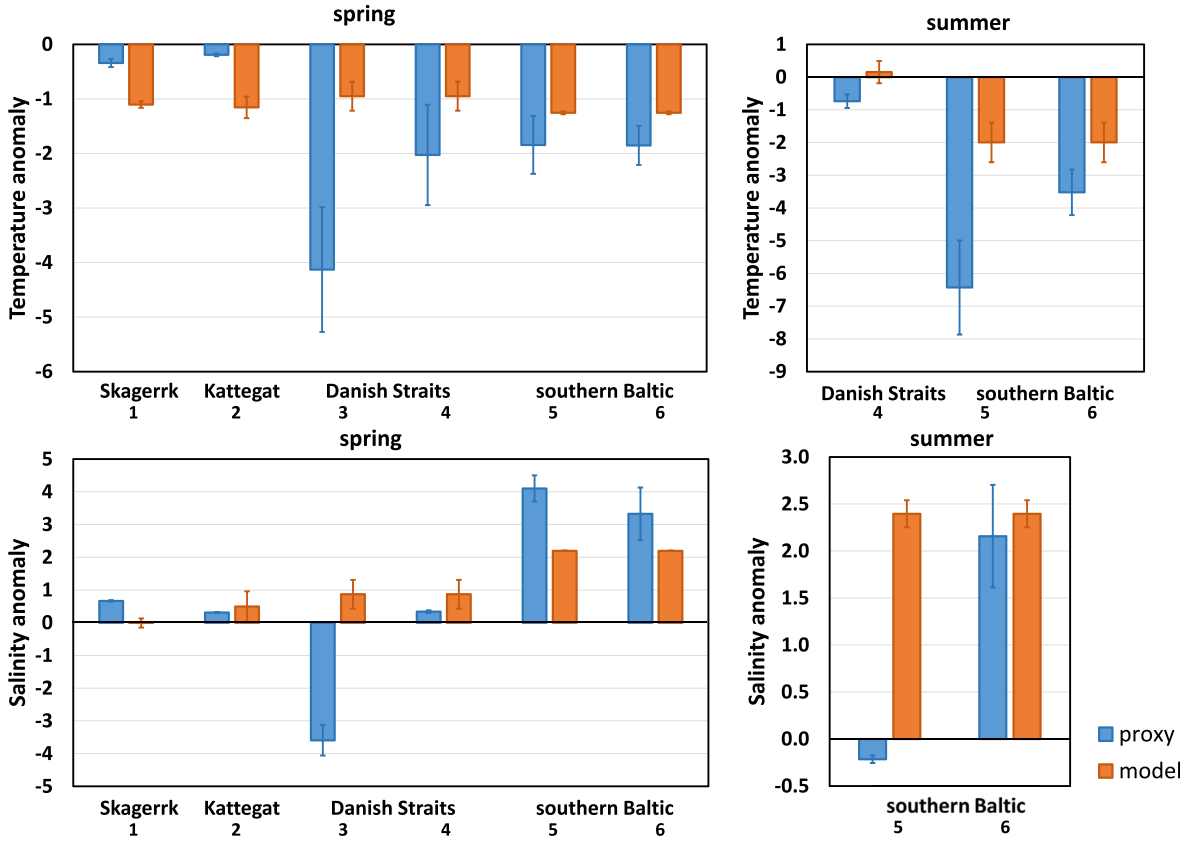

Fig. 10. Proxy–based and model simulations (LIG–$PD_{transient}$) of spring (MAM) and summer (JJA) of bottom water temperature and salinity anomalies at six sites (indicated by green numbers in Fig.1; the Skagerrak: 1) Åsted Vest; the Kattegat: 2) Anholt; the Danish Straits: 3) Mommark, 4) Ristinge; the southern Baltic: 5) Licze, 6) Obrzynowo. Error bars indicate one standard deviation.

different water depth sensitivity of data and model. Although topography changes were not included in the model, the agreement between the model simulation and proxy data highlights the potential influence of orbital and GHG settings on water thermal conditions in the North Sea–Baltic Sea transition zone and the Baltic Sea during different interglacial periods.

The simulated SST patterns exhibit greater similarities to the mean temperature of central Europe (Kühl and Litt, 2003) than to the northern Finland and the Nordic Seas (Kaspar et al., 2005; Bauch et al., 1999; Irvalı et al., 2012; Salonen et al., 2018). This suggests increased sensitivity to the Baltic Sea sea-ice and potential meltwater influences at northern high latitudes. In the Baltic Sea, the simulated sea-ice front reached around 60° N (Supplementary Fig. 4), meaning that the Baltic Proper and the southern Baltic Sea could have experienced minor influence from seasonal variations in sea-ice volume. Besides insolation influences, other factors such as circulation changes and the influx of warm water due to the wider opening in the Danish Straits and higher sea level during the first half of the LIG, also played significant roles in the amplitude of the seasonal cycle detected in the proxy reconstructions.

4.2.2. Salinity

Studies on paleo marine environments in the Kattegat at 125 ka BP suggest that the SSS was higher during the LIG. This conclusion is based on studies of gastropod $\delta^{18}O$ (Burman and Påsse, 2008), mollusc faunas (Funder et al., 2002), and diatom and dinoflagellate cyst (Head et al., 2005; Knudsen et al., 2012). These reconstructions indicate a higher SSS during the LIG, which is in overall agreement with our model simulations. In the transition zone and the southern Baltic Sea, the reconstructed and simulated BWSs in spring and summer generally agree, showing a range of 0–4. However, at two specific sites: Mommark in the Danish Straits and the site Licze in the southern Baltic, the reconstructed BWSs were lower during the LIG compared to those of the PD_{obs} (Ni et al., 2021, Fig. 10). The site Licze was located near to river mouths, which would have had a significant impact on freshwater input during the LIG. At Mommark, the benthic foraminifera species *Elphidium clavatum* was the dominant species, whereas the species *Ammonia batava*, which prefers shallower and less saline environments, was less abundant (Kristensen and Knudsen, 2006). This suggests that the water at Mommark was deeper compared to the nearby site Ristinge in the Danish Straits. The water depth at Mommark was ~22 m in the model simulations. The disagreement of proxy reconstructed and simulated BWS (Fig. 10, Danish Straits 1) indicates that at site Mommark, deeper waters (over 22 m) were required to reach a negative BWS LIG–$PD_{transient}$ anomaly, which agrees with the previous fauna assemblage results (Kristensen and Knudsen, 2006). When comparing BWS conditions, it is important to consider different water depths during various time periods in coastal areas. During summer, the site Licze - an estuary of the Vistula River - was more affected by river input than the southern Baltic Sea. This led to fresher bottom water conditions despite the more negative P–E in the LIG.

During the LIG, the Baltic Sea in general experienced significantly higher salinity levels than today, mainly due to a more open connection to the North Atlantic Ocean and a gradual increase in water depth over time (Seidenkrantz et al., 2000; Head et al., 2005; Knudsen et al., 2012; Ni et al., 2021). This connection which linked

to both the isostatic depression of the area from the penultimate glaciation and the higher sea-level during the LIG (Seidenkrantz et al., 2000) allowed for more marine water input, resulting in a more saline Baltic Sea environment. Even though our model does not account for such topographical changes of deeper waters and wider sea connections, the simulations show similar results, i.e., a more saline transition zone and the Baltic Sea in LIG. However, the model's accuracy may be influenced by these factors.

The increased exchange of saline and brackish water between the North Sea and the Baltic Sea during the LIG likely contributes to deep water formation in the eastern and central parts of the Baltic Sea. This, in turn, may have enhanced deep water ventilation. Moreover, proxy-based BWS reconstructions from the southern Baltic coastal area indicate a greater seasonality than our simulation suggests, particularly during spring and summer (Ni et al., 2021). This discrepancy could be due to the seasonal water depth changes.

4.3. Implications of the LIG environment in the North Sea–Baltic Sea region

4.3.1. Temperature changes

Simulations and proxy reconstructions show larger differences between SST and BWT during the LIG warm months (e.g., Jun–Oct), suggesting a more robust thermocline compared to the PD. The reconstructed BWT agrees with the simulations, demonstrating a lower BWT during the LIG in both spring and summer. This is mainly ascribed to higher GHG levels in the PD, even though the LIG had the stronger summer insolation. In converse, at the shallower sites (20–25 m water depth) in the transition zone (the Kattegat and the Danish Straits), the BWT anomalies reveal warmer summer conditions during the LIG. This suggests that insolation was the dominant factor affecting BWT at water depths less than 20–25 m.

The SST of the LIG was higher in summer and lower in winter compared to that of the PD, which can be attributed to the insolation variations during those months (Supplementary Fig. 1). Lower winter SST in the LIG was due to decreased winter insolation and lower GHG levels during the LIG compared to the PD. Comparing the LIG to PD and the LIG to PI water temperature anomalies highlight the impact of anthropogenic GHG. The annual mean temperature anomalies of LIG–PI were 2–3 °C higher than those for LIG–PD at the eight key locations (Fig. 6). This difference can be attributed to the elevated GHG concentration (CO_2: 124%, N_2O: 211%, CH_4: 113%) in the PD due to human activities compared to the conditions in the PI period.

However, stronger insolation fluctuations during the LIG resulted in pronounced seasonal temperature variations and a much higher summer SST compared to both the PI and the PD. Temperature anomalies of LIG–PD show significant inverse correlations with the P–E in the Kattegat, the Skagerrak, and the southern Baltic. More negative P–E anomalies during summer indicate drier conditions with higher evaporation and/or lower precipitation at the Baltic Sea entrance during the LIG.

This seawater temperature and P–E relationship does not apply to the open ocean area (the North Atlantic, the Norwegian Sea, and the North Sea) and the Baltic Proper, suggesting different P–E patterns for oceanic and terrestrial climates. In open ocean areas, the LIG-PD SST anomaly positively correlated with P–E, indicating that higher SST led to increased moisture and more precipitation.

Compared to the North Sea and open ocean area, the Baltic Sea displays a higher sensitivity to heat content changes in response to wind forcing (Schrum and Backhaus, 1999). An enhanced NAO during the LIG led to enhanced winter convection and westerlies, as a consequence of a weaker winter thermocline (smaller ΔT, Supplementary Fig. 2) compared with that during summer in the brackish water-dominated Baltic region (Schrum and Backhaus, 1999) during the LIG. Enhanced heat exchange between the sea surface and bottom water was expected during the LIG winter in the Baltic Sea.

4.3.2. Salinity changes

Seasonal variations in SSS and BWS in the Skagerrak and the transition zone are larger compared to those in the open ocean area and Baltic Proper. This is due to their relatively shallower water depth and unique locations, where a mix of marine and brackish water occurs. The water depth used in the simulations significantly influences water temperature and salinity results, and their amplitude variations in the coastal region and transition zones.

The disagreement between proxy reconstructions and model simulations of LIG–PD BWS at site Mommark, the Danish Straits may be partly attributed to the differences in water depth. Lower SSS during summer in these regions, along with lower P–E (higher evaporation and/or lower precipitation) suggests that P–E does not directly control SSS. Slightly lower salinity in the open ocean area (Fig. 5) during the LIG compared with that of the PD could be due to reduced sea-ice extent and thickness during the LIG (Supplementary Fig. 4) rather than the direct P–E effect. The AMOC simulations (EC-Earth3-LR, Zhang et al., 2021) and findings of warmer waters (Seidenkrantz et al., 2000; Grøsfjeld et al., 2006; Galaasen et al., 2014; Irvalı et al., 2012) indicate a stronger AMOC during the LIG compared with that of the PI, which would impact the temperature and salinity. The ocean circulation plays a more decisive role in affecting salinity of LIG-PI in the North Atlantic – North Sea region comparing with the direct effects of sea-ice content and P–E. The higher salinity during the LIG than that of the PI in the open ocean area in our simulations is likely ascribed to a stronger AMOC and more salty Atlantic water transported northward to the North Sea area.

The NAO may mainly control SSS in the transition zones, resulting in higher winter SSS due to increased saline water input from the North Sea into the Baltic Sea during positive winter NAO phases and increased freshwater outflow from the Baltic Sea in summer. The LIG–PI NAO anomalies show significant positive correlations with SSS and BWS anomalies in the transition area (the Kattegat and Danish Straits). During the LIG, a predominantly positive NAO index during cold seasons, particularly in October, may have played a crucial role in increasing westerlies and associated North Atlantic saline water inflow into the Baltic Sea compared to the PI. This would result in more wind-driven major inflows into the Baltic Sea and more intensive water exchange between the North Sea and the Baltic Sea during the LIG.

Near sea surface wind pattern anomalies (LIG–PI) during winter, mostly in November and December, show stronger westerlies in the LIG, resulting in increased saline water input through the Baltic Sea entrance (Supplementary Fig. 7a) compared to that in the PI. However, correlations between NAO and salinity anomalies of LIG–PD are not significant. The westerly anomalies of LIG-PD were not the dominant factor (Supplementary Fig. 7b), indicating that the differences in salinity between the LIG and the PD are affected by multiple factors that mask a clear NAO influence (such as strong GHG effects), while the differences between the LIG and the PI are mainly controlled by NAO variations. The differences between BWSs between LIG–PI and LIG–PD are not significant in the Kattegat, the Danish Straits, and the Baltic Proper, but are significant at other locations. This suggests that GHG-related climate changes during the PD acted as a non–dominant controlling factor for BWS at the Baltic–North Sea entrance and the inner Baltic Sea.

4.3.3. Precipitation-evaporation changes

The simulated P–E during the LIG was lower than that of the PD,

indicating higher evaporation than precipitation in the LIG. Simulated modern P–E in the Baltic Sea shows positive values, consistent with long–term (1981–1994) means of precipitation and evaporation estimates for various Baltic Sea regions, including the Kattegat and the Danish Straits (Omstedt et al., 1997).

There is no significant seasonal P–E fluctuation in LIG–PI anomalies, suggesting that factors such as insolation, temperature, and NAO had a minor impact on the P–E in the region. However, the P–E during the LIG and PD show significant differences, mainly due to a more positive PD P–E and stronger seasonal variations.

The P–E varied across different locations, such as land and sea. In open sea areas, such as the North Atlantic to the Norwegian Sea, the winter P–E of the PD was higher than that of the LIG and the PI, indicating a relatively wetter winter during the PD. In the coastal area, such as the Kattegat, Danish Straits, and the southern Baltic, the PD summer/autumn P–E displays more positive values compared to those in the LIG, indicating wetter summer/autumn conditions in coastal regions compared to the LIG. The relatively drier atmospheric conditions with less precipitation compared to evaporation in LIG summer, especially in the transition zone and the southern Baltic Sea, are related to warming over the Baltic Sea and westward advection of moisture from the Baltic Sea to the more open ocean. In open ocean regions, such as the North Atlantic, the North Sea, and the Norwegian Sea, the P–E impact on seawater salinity was minimal.

5. Conclusions

We focused on snapshot simulations in the LIG (127 ka BP), PI (1850 CE), and PD (1990 CE), examining seawater temperature, salinity, and their interactions with the P–E, sea-ice and NAO at eight key locations. We combined model simulations and proxy–based reconstructions to investigate the seawater conditions in the Baltic Sea – North Sea region during the LIG, and compared these findings with the modern ($PD_{transient}$, 1976–2005 CE for model simulation and PD_{obs}, 1990 CE for proxy-data) environment.

Our findings highlight the effects of stronger seasonal insolation variations during the LIG and elevated greenhouse gas concentrations during the PD. This suggests a greater seasonal variation of seawater conditions in the North Sea–Baltic Sea transition zone during the LIG, primarily due to stronger summer solar insolation.

The simulated monthly sea surface and bottom water temperature and salinity for the same locations at ~127 ka BP are generally in agreement with proxy-based reconstructions from the same time slice. The water temperature reconstructions based on the geochemistry of fossils reveal higher summer sea surface temperature (SST) and lower bottom water temperature (BWT) during the LIG. This suggests a more pronounced thermocline in the transition zone, which includes the Kattegat and the Danish Straits, compared to that of the PD. These findings are supported by the model simulations, and similar patterns were observed in both the North Atlantic and Baltic Sea regions.

The reconstructed and simulated bottom water salinity (BWS) data agree that during the LIG, the transition zone and the Baltic Sea experienced higher salinity levels in both spring and summer compared to that of the PD. Sea surface salinity (SSS) reconstructions in the Kattegat also indicate higher salinity levels during the LIG, which aligns with simulation results. The smaller salinity differences between surface– and bottom–waters during the LIG summer suggest a weaker halocline in the North Sea–Baltic Sea region compared to today. The discrepancy between proxy reconstructed and simulated BWS at the Danish Straits may stem from different water depths, but further research with more proxy data and higher resolution models incorporating LIG topography are necessary for a more thorough investigation.

The significant inverse correlation between SST and P–E at the Baltic entrance indicates that seawater temperature impacted the P–E patterns in the Skagerrak, the Kattegat, and the southern Baltic. The greater density difference in the water column during the LIG summer primarily due to the enhanced thermocline could have led to stronger stratification and hypoxic bottom water conditions. Higher SSS levels in the transition zone and southern Baltic Sea, along with more negative P–E values, imply a more arid environment in these regions during the LIG summer compared to the PD.

LIG–PI NAO anomalies show significant positive correlations with SSS anomalies in the transition area. A predominantly positive NAO phase during the LIG winters, most notably in October, may explain a substantial portion of the higher salinities in the Baltic Sea.

Author contribution

S. Ni: Conceptualization, Methodology, Writing – original draft, Writing – review & editing, Funding acquisition, Visualization, Investigation, Formal analysis. Z. Lu: Conceptualization, Methodology, Investigation, Writing – review & editing. Q. Zhang: Conceptualization, Methodology, Investigation, Writing – review & editing. J. Groeneveld: Writing – review & editing, Formal analysis. K.L. Knudsen: Writing – review & editing. M.-S. Seidenkrantz: Writing – review & editing, Funding acquisition, Project administration. H.L. Filipsson: Conceptualization, Writing – review & editing, Supervision, Funding acquisition, Project administration

Declaration of competing interest

The authors declare that they have no known competing financial interests or personal relationships that could have appeared to influence the work reported in this paper.

Data availability

Datasets related to this article are available at:Ni, Sha (2023), “Last interglacial seasonal hydroclimate in the North Sea–Baltic Sea region”, Mendeley Data, V1, doi: https://doi.org/10.17632/dg8kgfbphy.1.

Acknowledgments

We thank the strategic research area MERGE (Modeling the Regional and Global Earth system) at the Centre for Environmental and Climate Research (CEC), Lund University for funding. We acknowledge support from the Swedish Research Council (2022-03129). Simulations with EC–Earth were performed on resources provided by the Swedish National Infrastructure for Computing (SNIC) at the National Supercomputer Centre (NSC) partially funded by the Swedish Research Council through grant agreement no. 2022-06725 and no. 2018-05973. The SMHI hydrographic data collection is organized by the environmental monitoring program and funded by the SwAM. We also acknowledge the Independent Research Fund Denmark (grant no. 0135–00165B (GreenShelf) to MSS); the project has also received funding from the European Union's Horizon 2020 research and innovation program under grant agreement no. 869383 (ECOTIP) (MSS).

Appendix A. Supplementary data

Supplementary data related to this article can be found at https://doi.org/10.1016/j.quascirev.2023.108152.

References

Adkins, J.F., Boyle, E.A., Keigwin, L., Cortijo, E., 1997. Variability of the North Atlantic thermohaline circulation during the last interglacial period. Nature 390 (6656), 154–156.

Bauch, H.A., Erlenkeuser, H., Fahl, K., Spielhagen, R.F., Weinelt, M.S., Andruleit, H., Henrich, R., 1999. Evidence for a steeper Eemian than Holocene sea surface temperature gradient between Arctic and sub–Arctic regions. Palaeogeogr. Palaeoclimatol. Palaeoecol. 145 (1–3), 95–117.

Bereiter, B., Eggleston, S., Schmitt, J., Nehrbass-Ahles, C., Stocker, T.F., Fischer, H., Kipfstuhl, S., Chappellaz, J., 2015. Revision of the EPICA Dome C CO_2 record from 800 to 600 kyr before present. Geophys. Res. Lett. 42 (2), 542–549.

Berger, A., 1978. Long–term variations of daily insolation and Quaternary climatic changes. J. Atmos. Sci. 35 (12), 2362–2367.

Berger, A., Loutre, M.-F., 1991. Insolation values for the climate of the last 10 million years. Quat. Sci. Rev. 10 (4), 297–317.

Bova, S., Rosenthal, Y., Liu, Z., Godad, S.P., Yan, M., 2021. Seasonal origin of the thermal maxima at the Holocene and the last interglacial. Nature 589 (7843), 548–553.

Brocas, W.M., Felis, T., Obert, J.C., Gierz, P., Lohmann, G., Scholz, D., Kölling, M., Scheffers, S.R., 2016. Last interglacial temperature seasonality reconstructed from tropical Atlantic corals. Earth Planet Sci. Lett. 449, 418–429.

Burman, J., Påsse, T., 2008. Oceanography in northwestern Europe during the last interglacial from intrashell $\delta^{18}O$ ranges in Littorina littorea gastropods. Quaternary Research 70 (1), 121–128.

Caian, M., Koenigk, T., Döscher, R., Devasthale, A., 2018. An interannual link between Arctic sea–ice cover and the North Atlantic Oscillation. Clim. Dynam. 50 (1–2), 423–441.

Cortijo, E., Lehman, S., Keigwin, L., Chapman, M., Paillard, D., Labeyrie, L., 1999. Changes in meridional temperature and salinity gradients in the North Atlantic Ocean (30–72 N) during the last interglacial period. Paleoceanography 14 (1), 23–33.

Döscher, R., Acosta, M., Alessandri, A., Anthoni, P., Arsouze, T., Bergman, T., Bernardello, R., Boussetta, S., Caron, L.P., Carver, G., Castrillo, M., 2022. The EC-earth3 Earth system model for the coupled model Intercomparison project 6. Geosci. Model Dev. (GMD) 15 (7), 2973–3020.

Felis, T., Lohmann, G., Kuhnert, H., Lorenz, S.J., Scholz, D., Pätzold, J., Al–Rousan, S.A., Al–Moghrabi, S.M., 2004. Increased seasonality in Middle East temperatures during the last interglacial period. Nature 429 (6988), 164–168.

Fronval, T., Jansen, E., Haflidason, H., Sejrup, H.P., 1998. Variability in surface and deep water conditions in the Nordic seas during the last interglacial period. Quat. Sci. Rev. 17 (9–10), 963–985.

Funder, S., Demidov, I., Yelovicheva, Y., 2002. Hydrography and mollusc faunas of the baltic and the white Sea–North sea seaway in the eemian. Palaeogeogr. Palaeoclimatol. Palaeoecol. 184 (3–4), 275–304.

Funder, S., Balic-Zunic, T., 2006. Hypoxia in the Eemian: mollusc faunas and sediment mineralogy from Cyprina Clay in the southern Baltic region. Boreas 35 (2), 367–377.

Galaasen, E.V., Ninnemann, U.S., Irvalı, N., Kleiven, H.K.F., Rosenthal, Y., Kissel, C., Hodell, D.A., 2014. Rapid reductions in North Atlantic Deep Water during the peak of the last interglacial period. Science 343 (6175), 1129–1132.

Grøsfjeld, K., Funder, S., Seidenkrantz, M.-S., Glaister, C., 2006. Last interglacial marine environments in the White Sea region, northern Russia. Boreas 35, 493–520.

Hansson, D., Gustafsson, E., 2011. Salinity and hypoxia in the Baltic Sea since AD 1500. J. Geophys. Res.: Oceans 116 (C3).

Head, M.J., Seidenkrantz, M.S., Janczyk-Kopikowa, Z., Marks, L., Gibbard, P.L., 2005. Last Interglacial (Eemian) hydrographic conditions in the southeastern Baltic Sea, NE Europe, based on dinoflagellate cysts. Quaternary International 130 (1), 3–30.

HELCOM, 2018. State of the Baltic Sea – second HELCOM holistic assessment 2011-2016. Baltic Sea Environment Proceedings 155.

Humborg, C., Fennel, K., Pastuszak, M., Fennel, W., 2000. A box model approach for a long–term assessment of estuarine eutrophication, Szczecin Lagoon, southern Baltic. J. Mar. Syst. 25 (3–4), 387–403.

Hurrell, J.W., 1995. Decadal trends in the North Atlantic Oscillation: regional temperatures and precipitation. Science 269 (5224), 676–679.

Irvalı, N., Ninnemann, U.S., Galaasen, E.V., Rosenthal, Y., Kroon, D., Oppo, D.W., Kleiven, H.F., Darling, K.F., Kissel, C., 2012. Rapid switches in subpolar North Atlantic hydrography and climate during the Last Interglacial (MIS 5e). Paleoceanography 27 (2).

Kaspar, F., Kühl, N., Cubasch, U., Litt, T., 2005. A model-data comparison of European temperatures in the Eemian interglacial. Geophys. Res. Lett. 32 (11).

Knudsen, K.L., Jiang, H., Gibbard, P.L., Kristensen, P., Seidenkrantz, M.S., Janczyk-Kopikowa, Z., Marks, L., 2012. Environmental reconstructions of E emian S tage interglacial marine records in the L ower V istula area, southern B altic S ea. Boreas 41 (2), 209–234.

Kristensen, P.H., Knudsen, K.L., 2006. Palaeoenvironments of a complete Eemian sequence at Mommark, South Denmark: foraminifera, ostracods and stable isotopes. Boreas 35 (2), 349–366.

Kühl, N., Litt, T., 2003. Quantitative time series reconstruction of Eemian temperature at three European sites using pollen data. Veg. Hist. Archaeobotany 12 (4), 205–214.

Kuhlbrodt, T., Griesel, A., Montoya, M., Levermann, A., Hofmann, M., Rahmstorf, S., 2007. On the driving processes of the Atlantic meridional overturning circulation. Reviews of Geophysics 45 (2).

Lambert, E., Eldevik, T., Haugan, P.M., 2016. How northern freshwater input can stabilise thermohaline circulation. Tellus A: Dynamic Meteorology and Oceanography 68 (1), 31051.

Lambert, E., Eldevik, T., Spall, M.A., 2018. On the dynamics and water mass transformation of a boundary current connecting alpha and beta oceans. Journal of Physical Oceanography 48 (10), 2457–2475.

Laskar, J., Robutel, P., Joutel, F., Gastineau, M., Correia, A., Levrard, B., 2004. A long–term numerical solution for the insolation quantities of the Earth. Astron. Astrophys. 428, 261–285.

Lehmann, A., Hinrichsen, H.H., 2001. The importance of water storage variations for water balance studies of the Baltic Sea. Phys. Chem. Earth - Part B Hydrol., Oceans Atmos. 26 (5–6), 383–389.

Loulergue, L., Schilt, A., Spahni, R., Masson–Delmotte, V., Blunier, T., Lemieux, B., Barnola, J.M., Raynaud, D., Stocker, T.F., Chappellaz, J., 2008. Orbital and millennial–scale features of atmospheric CH 4 over the past 800,000 years. Nature 453 (7193), 383–386.

Lu, J., Greatbatch, R.J., 2002. The changing relationship between the NAO and northern hemisphere climate variability. Geophys. Res. Lett. 29 (7), 52-51–52-54.

Lu, Z., Zhang, Q., Miller, P.A., Zhang, Q., Berntell, E., Smith, B., 2021. Impacts of large-scale sahara solar farms on global climate and vegetation cover. Geophys. Res. Lett. 48 (2), e2020GL090789.

Mariotti, A., Arkin, P., 2007. The North Atlantic Oscillation and oceanic precipitation variability. Clim. Dynam. 28 (1), 35–51.

Massel, S.R., 2015. Internal Gravity Waves in the Shallow Seas. Springer International Publishing, Poland.

Ni, S., Krupinski, N.Q., Chonewicz, J., Groeneveld, J., Knudsen, K.L., Seidenkrantz, M.S., Filipsson, H.L., 2021. Seasonal climate variations in the Baltic Sea during the Last Interglacial based on foraminiferal geochemistry. Quat. Sci. Rev. 272, 107220.

Olsen, J., Anderson, J.N., Knudsen, M.F., 2012. Variability of the North Atlantic oscillation over the past 5,200 years. Nat. Geosci. 5, 808–812. https://doi.org/10.1038/ngeo1589.

Omstedt, A., Meuller, L., Nyberg, L., 1997. Interannual, Seasonal and Regional Variations of Precipitation and Evaporation over the Baltic Sea.Ambio, pp. 484–492.

Otto-Bliesner, B.L., Braconnot, P., Harrison, S.P., Lunt, D.J., Abe-Ouchi, A., Albani, S., Bartlein, P.J., Capron, E., Carlson, A.E., Dutton, A., Fischer, H., Goelzer, H., Govin, A., Haywood, A., Joos, F., LeGrande, A.N., Lipscomb, W.H., Lohmann, G., Mahowald, N., Nehrbass-Ahles, C., Pausata, F.S.R., Peterschmitt, J.-Y., Phipps, S.J., Renssen, H., Zhang, Q., 2017. The PMIP4 contribution to CMIP6 – Part 2: two interglacials, scientific objective and experimental design for Holocene and Last Interglacial simulations. Geosci. Model Dev. (GMD) 10 (11), 3979–4003. https://doi.org/10.5194/gmd-10-3979-2017.

Otto–Bliesner, B.L., Rosenbloom, N., Stone, E.J., McKay, N.P., Lunt, D.J., Brady, E.C., Overpeck, J.T., 2013. How warm was the last interglacial? New model–data comparisons. Philosophical Transactions of the Royal Society A. Math. Phys. Eng. Sci. 371 (2001), 20130097.

Salonen, J.S., Helmens, K.F., Brendryen, J., Kuosmanen, N., Väliranta, M., Goring, S., Korpela, M., Kylander, M., Philip, A., Plikk, A., Renssen, H., 2018. Abrupt high–latitude climate events and decoupled seasonal trends during the Eemian. Nat. Commun. 9 (1), 1–10.

Schrum, C., Backhaus, J.O., 1999. Sensitivity of atmosphere–ocean heat exchange and heat content in the North Sea and the Baltic Sea. Tellus 51 (4), 526–549.

Schilt, A., Baumgartner, M., Schwander, J., Buiron, D., Capron, E., Chappellaz, J., Loulergue, L., Schüpbach, S., Spahni, R., Fischer, H., Stocker, T.F., 2010. Atmospheric nitrous oxide during the last 140,000 years. Earth Planet Sci. Lett. 300 (1–2), 33–43.

Schimanke, S., Meier, H.E.M., Kjellström, E., Strandberg, G., Hordoir, R., 2012. The climate in the Baltic Sea region during the last millennium simulated with a regional climate model. Clim. Past 8, 1419–1433. https://doi.org/10.5194/cp-8-1419-2012.

Schneider, R., Schmitt, J., Köhler, P., Joos, F., Fischer, H., 2013. A reconstruction of atmospheric carbon dioxide and its stable carbon isotopic composition from the penultimate glacial maximum to the last glacial inception. Clim. Past 9 (6), 2507–2523.

Seidenkrantz, M.-S., Aagaard–Sørensen, S., Møller, H.S., Kuijpers, A., Jensen, K.G., Kunzendorf, H., 2007. Hydrography and climatic change during the last 4.400 years in Ameralik Fjord, SW Greenland. Holocene 17 (3), 387–401.

Seidenkrantz, M.-S., Knudsen, K.L., Kristensen, P.H., 2000. Marine Late Saalian to Eemian environments and climatic variability in the Danish area. Netherlands Journal of Geosciences, Geologie en Mijnbouw 79, 335–343.

Sicre, M.-A., Weckström, K., Seidenkrantz, M.-S., Kuijpers, A., Benetti, M., Massé, M., Ezat, U., Schmidt, S., Bouloubassi, I., Olsen, J., Khodri, M., Mignot, J., 2014. Labrador Current variability over the last 2000 years. Earth Planet Sci. Lett. 400, 26–32. https://doi.org/10.1016/j.epsl.2014.05.016.

Trigo, R.M., Osborn, T.J., Corte–Real, J.M., 2002. The North Atlantic Oscillation influence on Europe: climate impacts and associated physical mechanisms.

Climate research 20 (1), 9–17.
Trouet, V., Scourse, J.D., Raible, C.C., 2012. North Atlantic storminess and Atlantic Meridional overturning circulation during the last millennium: reconciling contradictory proxy records of NAO variability. Global Planet. Change 84–85, 48–55. https://doi.org/10.1016/j.gloplacha.2011.10.003.
Winsor, P., Rodhe, J., Omstedt, A., 2001. Baltic Sea ocean climate: an analysis of 100 yr of hydrographic data with focus on the freshwater budget. Climate Research 18 (1–2), 5–15.
Zhang, Q., Berntell, E., Axelsson, J., Chen, J., Han, Z., de Nooijer, W., Lu, Z., Li, Q., Zhang, Q., Wyser, K., Yang, S., 2021. Simulating the mid–Holocene, last interglacial and mid–Pliocene climate with EC–Earth3–LR. Geosci. Model Dev. (GMD) 14 (2), 1147–1169.